

Article

Investigating the Use of Sentinel-1 for Improved Mapping of Small Peatland Water Bodies: Towards Wildfire Susceptibility Monitoring in Canada's Boreal Forest

Samantha Schultz ¹, Koreen Millard ^{1,*} , Samantha Darling ¹ and René Chénier ²

¹ Department of Geography and Environmental Studies, Carleton University, 1125 Colonel by Drive, Ottawa, ON K1S 5B6, Canada; samantha.j.schultz@cmail.carleton.ca (S.S.)

² Canadian Hydrographic Service, 200 Kent Street, Ottawa, ON K1A 0E6, Canada

* Correspondence: koreen_millard@carleton.ca

Abstract: Peatlands provide vital ecosystem and carbon services, and Canada is home to a significant peatland carbon stock. Global climate warming trends are expected to lead to increased carbon release from peatlands, as a consequence of drought and wildfire. Monitoring hydrologic regimes is a key in understanding the impacts of warming, including monitoring changes in small and temporally variable water bodies in peatlands. Global surface water mapping has been implemented, but the spatial and temporal scales of the resulting data products prevent the effective monitoring of peatland water bodies, which are small and prone to rapid hydrologic changes. One hurdle in the quest to improve remote-sensing-derived global surface water map quality is the omission of small and temporally variable water bodies. This research investigated the reasons for small peatland water body omission as a preparatory step for surface water mapping, using Sentinel-1 SAR data and image classification methods. It was found that Sentinel-1 backscatter signatures for small peatland water bodies differ from large water bodies, due in part to differing physical characteristics such as waves and emergent vegetation, and limitations in detectable feature sizes as a result of SAR image processing and resolution. The characterization of small peatland water body backscatter provides a theoretical basis for the development of SAR-based surface water mapping methods with high accuracy for our purposes of wildfire susceptibility monitoring in peatlands. This study discusses the implications of small peatland water body omission from surface water maps on carbon, climate, and hydrologic models.

Keywords: peatland; surface water; Sentinel-1



Citation: Schultz, S.; Millard, K.; Darling, S.; Chénier, R. Investigating the Use of Sentinel-1 for Improved Mapping of Small Peatland Water Bodies: Towards Wildfire Susceptibility Monitoring in Canada's Boreal Forest. *Hydrology* **2023**, *10*, 102. <https://doi.org/10.3390/hydrology10050102>

Academic Editor: Giorgio Baiamonte

Received: 17 March 2023

Revised: 24 April 2023

Accepted: 25 April 2023

Published: 27 April 2023



Copyright: © 2023 by the authors. Licensee MDPI, Basel, Switzerland. This article is an open access article distributed under the terms and conditions of the Creative Commons Attribution (CC BY) license (<https://creativecommons.org/licenses/by/4.0/>).

1. Introduction

1.1. Hydrologic Variability and Wildfires in Peatlands

Peatlands are ecologically significant wetland habitats with unique vegetation, soil structure, and low rates of decomposition, which facilitate the accumulation of carbon. Subarctic and boreal peatlands, the dominant types found in Canada [1], store up to 30% of global soil carbon, making them a significant global peatland carbon stock [2]. The long-term carbon storage capabilities of peatlands means that they play a crucial role in the global carbon cycle [3]. When this process is disrupted by drought, fire, or human activities, the impacts to the carbon budget are severe [3–5].

Peatland hydrology is complex, affected by local weather conditions, long-term weather trends, human activities, and topography [6]. In turn, peatland hydrology influences rates of peat development and the ability of the peatland to perform ecosystem services such as carbon storage [3]. Peatlands with high moisture retention capabilities and a moderated water table are resilient to wildfire and offset carbon loss post-fire [7]. Peat fires are capable of smoldering for years, due to the large accumulation of organic matter for fuel [8,9]. Peatlands that experience fire may become and remain vulnerable to repeat

fire events due to global warming trends; drier conditions increase the risk of wildfire and the severity of the burn [3,7,10–13]. The availability of water may be influenced by global temperature increases, which will lead to an increased prevalence of drought [11,12] and potentially extreme weather [14,15]. In turn, the risk of wildfires is greatly increased due to dry vegetation and soil becoming available for surface fuel [9]. The increased frequency of lightning storms results in more chances for ignition [15,16], and peatlands become more vulnerable due to drier conditions [7,13]. In general, wildfires are a costly disturbance. Air quality declines near wildfires, as well as in downwind regions, producing haze and decreasing the amount of incident solar radiation. As a consequence of these effects, the CO₂ uptake by vegetation is suppressed due to reduced sunlight for photosynthesis, further exacerbating the problem of carbon dioxide emissions due to fire [17,18]. In peatlands, the volume of carbon emissions is even greater due to the immense volumes of carbon dioxide and methane stored in peat [3,4,19]. Peatland wildfires are hazardous to human health as a result of the widespread effects of air pollution and water pollution, due to peatland's connectivity with water systems [18,20,21].

1.2. Fire Danger Monitoring with Remote Sensing

Monitoring infrastructure is limited in Northern Canada, due to low population and logistical constraints such as economic feasibility. Therefore, conditions in peatlands are poorly represented in meteorologic data due to the reliance on interpolated data from sparse meteorological stations [22]. Considering the global implications of peatland ecosystem services and the limitations of existing data sources it is clear that new methods must be established to continuously monitor conditions in peatlands. Forest fire danger rating systems are tools used by agencies to assess moisture conditions and guide fire management decisions [23]. The Canadian Forest Fire Danger Rating System (CFFDRS) is widely used [23], for which the contributing indices are derived solely from meteorological data. This system is not accurate across all ranges of peat properties, making it unreliable for broad application in Canada's peatlands [22].

In order to monitor fire danger in peatlands, we need a method that is more suited to remote areas. Additionally, most danger rating systems are designed for forests dominated by vascular vegetation [24,25]. Peatlands differ from forests in structure and plant life; *Sphagnum* mosses, which are a common plant in peatlands, are not vascular [26]. Water variability is a better indicator of peatland drought [22]. Open water bodies in peatlands have been observed to grow or shrink in size with changes in water availability. Monitoring the dynamics of these ponds would improve the quality of fire danger rating systems for peatland environments. In order to fully understand the hydrologic regimes of Canada's peatlands in an effort to mitigate wildfire risk, high-quality surface water maps with high temporal resolution are required. Presently, near-real-time surface water products that capture small peatland water bodies do not exist.

1.3. Surface Water Mapping with Remote Sensing

The European Commission Joint Research Centre's Global Surface Water (GSW) products are generated using the Landsat archive, with the goal of mapping the long-term temporal variability of surface water [27]. The GSW products are spatially coarse (30 m resolution) and not temporally specific, due to aggregation of data across the entire Landsat reserve [27]. The GSW Water Occurrence product, showing where water occurs between 1984 and 2021, does not capture ephemeral or seasonal water bodies well; most peatland water bodies are omitted. Shallow and temporally dynamic water bodies are often omitted in optical-based surface water classifications as a result of coarse resolution or misclassification.

Generally, optical data are thought to be less effective than synthetic aperture RADAR (SAR) at differentiating water from land, especially shallow or vegetated water bodies, due to confusion between saturated soil or vegetation and water. In order to improve upon existing surface water products, we should turn to SAR-based methods. SAR uses active

microwaves that are impervious to cloud and weather effects, and free and open datasets are available on a biweekly basis (Sentinel-1). Sentinel-1 has been collecting data since 2016, and will continue to provide coverage over Canada, so it is a reliable option for operational mapping [28].

SAR is regularly used for hydrologic mapping applications, as microwave signals are highly sensitive to water content, allowing for easy distinction between hydrologic features and saturated soils (e.g., [24]). Water produces specular reflectance in SAR backscatter, with pronounced differences from many land cover types, making SAR an ideal data source for producing high-quality surface water maps. We expect the backscatter coefficient to increase as soil wetness increases, up until the surface is inundated with water, at which point specular reflectance leads to very low backscatter return that is typically below the sensor's noise floor (Figure 1). Inundation occurs when the water table exceeds ground surface level (>0 cm), because there is no penetration of microwaves into water.

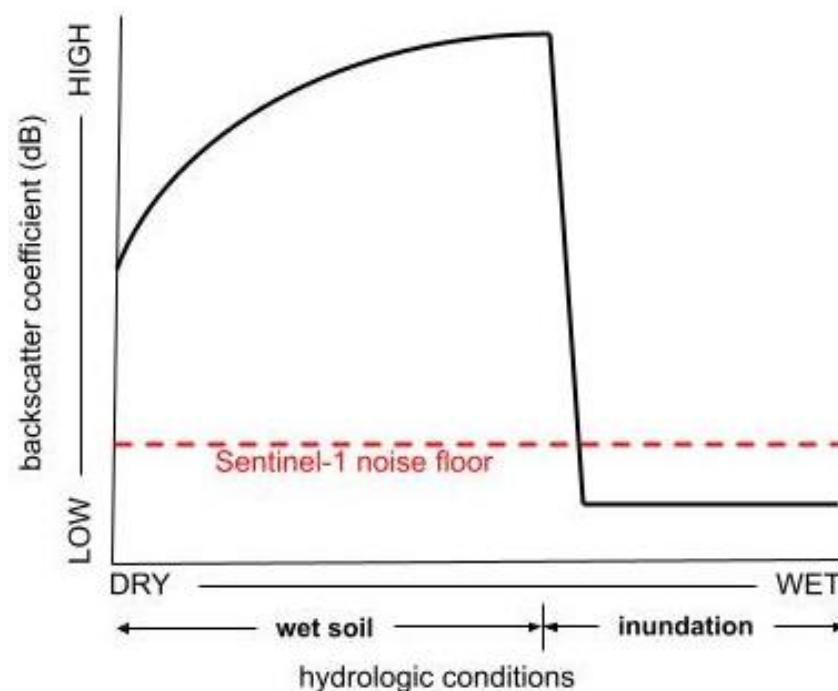


Figure 1. Theoretical relationship between Sentinel-1 backscatter and water. Sentinel-1 noise floor is indicated by the dashed line (−22 dB). Adapted from [29].

SAR threshold-based classification is simple, but often leads to errors of omission for the water class; it requires an analyst to set unique thresholds for each image to help the algorithm distinguish water from land [30–32]. Machine learning-powered SAR surface water maps have been highly successful [24,25]; however, the preliminary results of SAR-based image classification for water extent mapping indicated that small peatland water bodies pose unique problems. Characterizing the SAR response of small peatland water bodies enables the development of SAR-based surface water mapping methods with high accuracy.

Many environmental monitoring applications would benefit from high-resolution, reliable, and temporally specific surface water maps. Climate models that make use of surface water data could improve inputs for simulating water in the biogeochemical pathways involved in climate, such as evaporation. Monitoring peatlands via high-resolution surface water maps could provide an indicator of peat drying [33], which may help to quantify both carbon dioxide exchange and methane release. Water resource management and emergency management could be improved by spatially and temporally specific surface water data, enhancing current capabilities of predicting water supply and flood risk. For our intended purpose of improving drought detection in peatlands, high-quality surface water maps,

in combination with soil moisture data and meteorological data, could improve drought detection in peatlands and benefit peatland conservation efforts.

1.4. Research Objectives

As open standing water is known to produce specular reflectance in SAR backscatter, we initially hypothesized that all water bodies that are larger than the spatial resolution of the SAR sensor would produce the same low backscatter response as larger water bodies (i.e., those captured in the GSW dataset). In a preliminary investigation, we tested image classification techniques and used the GSW dataset to automatically create training data. In these preliminary results, small water bodies were not captured in the resulting classified maps. We hypothesized that this indicated that water bodies of a certain size exhibit a different backscatter signature than larger water bodies. Therefore, the objectives of this research were as follows:

1. Determine if there is a significant difference in SAR backscatter between large and small peatland water bodies;
2. Assess any relationship between peatland water body size and backscatter intensity.

2. Materials and Methods

Across a set of randomly selected peatland sites, water bodies that were not captured by the GSW dataset were digitized from high-resolution imagery at three time periods throughout the ice-free season of 2021. Examining the same sites across three dates allows for the assessment of change and a characterization of changes in the size, disappearance, or emergence of water bodies.

2.1. Site Selection and Digitizing

To sample peatland water bodies across the boreal forest, a set of 100 random points (henceforth called “sites”) were generated throughout the area covered by the Enhanced Wetland Classification [34] for the Boreal Forest provided by Ducks Unlimited Canada (Figure 2). This map differentiates between peatland and non-peatland wetlands, as well as burned and upland areas. The open water class in this map product is not temporally specific (i.e., the date of the exact water extent for any given pixel is unknown). Each sample point was buffered to a 0.5 km radius, and the resulting circle was bounded by a square to generate a 1 km² site.

For each site, high-resolution (3.7 m pixel spacing) PlanetScope SuperDove [35] optical imagery was obtained for late May (nearest image available to 25 May), early July (nearest image available to 5 July), and late September (nearest image available to 25 September), using the Planet’s Education and Research access program. At each site and for each date, open water bodies that did not appear in the GSW occurrence product as permanent water, which had a 90% occurrence or greater [24], were digitized manually using SuperDove imagery. The result was three datasets representing small peatland water bodies in May, July, and September, 2021.

To facilitate a comparison of Sentinel-1 backscatter values at two polarizations (VV and VH) to water body size, a separate sample of 200 large and permanent water bodies in the region of the DUC Enhanced Peatland Classification, identified using the GSW occurrence dataset where occurrence is stable (occurrence estimated to be greater than 90%), was also digitized using SuperDove optical imagery in the summer of 2021. The precise date was not important to the analysis, as this class represents permanent water bodies for which the configuration rarely changes.

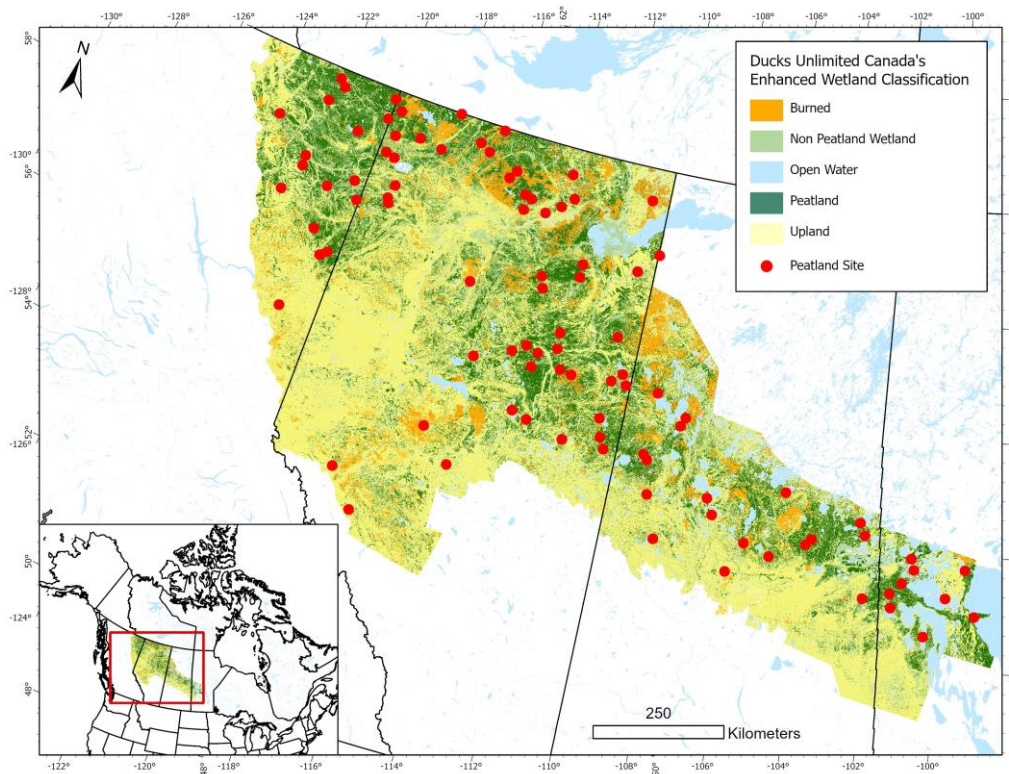


Figure 2. Ducks Unlimited Canada’s Enhanced Wetland Classification, with 100 sites randomly generated on peatland [34].

Sentinel-1 interferometric wide ground range imagery (10 m pixel spacing) was accessed using Google Earth Engine, which was pre-processed using thermal noise removal, radiometric calibration, and terrain correction using SRTM 30 [36,37]. Additional terrain correction was not performed, due to low topographic variations in peatlands. A Refined Lee speckle filter (3×3 window size) was applied to the images prior to extraction [38].

2.2. Data Extraction

To create datasets from which to sample Sentinel-1 backscatter, a point was generated at the centroid for each digitized water body. Pre-selection of the centroid of the water bodies helps mitigate the risk of a randomly sampled pixel being located on the edge of a water body, which would cause contamination between water and land classes. The result was three datasets representing the center points of small peatland water bodies in May, July, and September, 2021 (Figure 3). For the additional large water body dataset, the area was computed, and a centroid was generated for each large water body to be used for Sentinel-1 backscatter data extraction.

Using these three sets of data, VV and VH backscatter values were extracted from Sentinel-1 imagery at dates that closely corresponded to the three dates of small water body digitizing. There was never greater than 9 days between the date of the image used for digitizing and the date of Sentinel-1 data extraction. This was important to reduce the risk of a peatland water body changing in size or disappearing between the two images. The ranges of dates required to obtain full coverage of all sites for each study date are as follows:

- Late May–20 May to 29 May 2021;
- Early July–1 July to 10 July 2021;
- Late September–20 September to 29 September 2021.

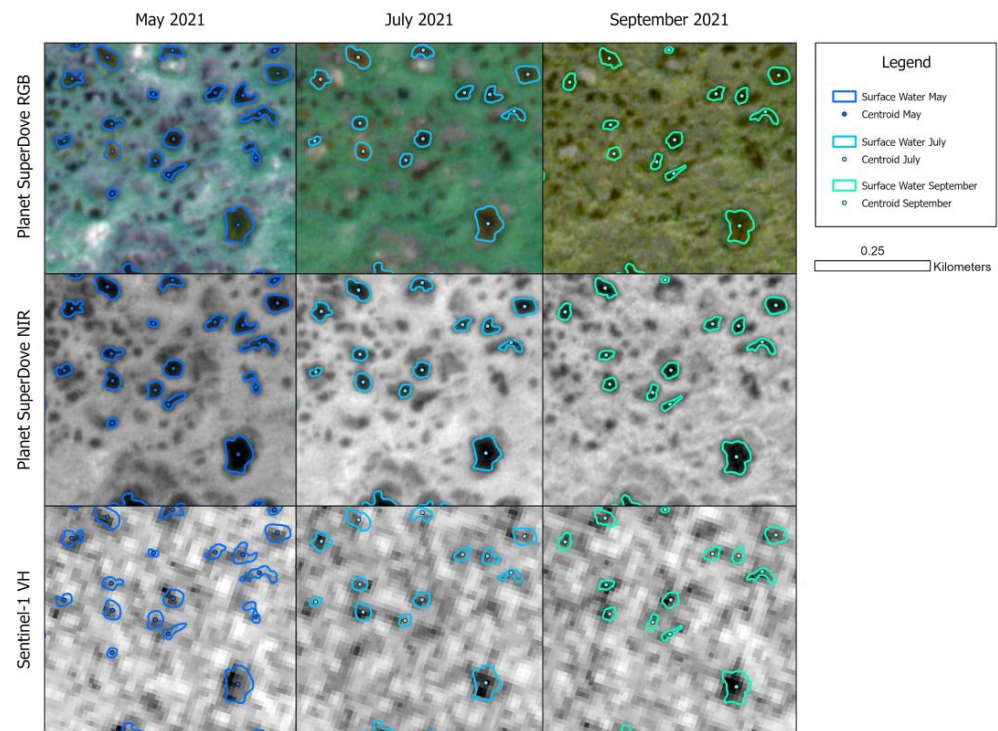


Figure 3. Small digitized water bodies in an example peatland site. Polygons represent the water extent at each of the three study dates. Points represent the centroids of the water bodies. The top row is underlain by PlanetScope SuperDove imagery displayed in RGB, and the second row by the same PlanetScope imagery displayed in NIR, from 29 May, 6 July, and 21 September 2021, left to right. The bottom row is underlain by Sentinel-1 Interferometric Wide (IW) Ground Range- = Detected VH band from 27 May, 2 July, and 24 September 2021, respectively. The Global Surface Water dataset is not shown, as there was no water detected in this area.

The VV and VH backscatter intensity values, in decibels, were extracted for the pixels which intersected each of the three classes of points (small water body, large water body (captured in GSW), and land).

2.3. Analysis

2.3.1. Statistical Comparison of Backscatter

Using the extracted backscatter data, a Wilcoxon rank sum test (a non-parametric technique) was used to test the hypothesis that the small peatland water body and large GSW water body populations have equal medians [39]. If the null hypothesis is rejected, the small and large water bodies are statistically significantly different from each other. This hypothesis was assessed for VV backscatter and VH backscatter and several derivatives. VV/VH derivatives (polarized ratio, normalized difference polarized index, normalized VH index, normalized VV index) were calculated and tested for significant differences using a Wilcoxon rank sum test. These derivatives have been found to improve the distinction of open water from similar classes in surface water classifications [40]. The same analysis was performed to compare small peatland water bodies and land. A visual inspection of boxplots was used to compare the statistical distribution of backscatter values for small peatland water bodies, large GSW water bodies, and land. Histograms of the extracted data were generated to assess the feasibility of threshold-based classification methods.

2.3.2. Statistical Comparison of Water Body Sizes

The possibility of a relationship between backscatter and water body size was explored using scatterplots and linear regression analysis.

3. Results

3.1. Seasonal Patterns in Peatland Hydrology

The number and size of small digitized peatland water bodies differed between the three study dates. The minimum mapping unit was 100 m², or 10 × 10 m², because of the resolution of Sentinel-1 IW GRD images. The number of small peatland water bodies declined over time, and the average water body size declined between May and July, and between July and September (Table 1).

Table 1. Quantity and area statistics of small peatland water bodies in May, July, and September, 2021. The standard deviation is reported in brackets, along with the mean size.

Month	# of Small Water Bodies	Mean Size (m ²) (±σ)	Maximum Size (m ²)
May	225	2062 (±6685)	73,927
July	121	1571 (±7493)	64,245
September	87	1336 (±9425)	70,761

The distribution of small digitized peatland water bodies by size reveals that the smallest water bodies (<1000 m²) often disappeared between May and September, and the larger ones generally decreased in size. The single water body with the largest maximum area in May was 73,927 m², and this water body decreased to 64,245 m² in July but rebounded to 70,761 m² in September.

3.2. Sentinel-1 Backscatter Signatures of Small and Large Water Bodies

Small and large water bodies have statistically different VV and VH backscatter properties. The polarized ratio and the other VV/VH derivatives were also statistically different for small and large water bodies (Table 2). Small water bodies were statistically different from land for all variables in May and September. In July, only VV and VH were significantly different between land and small water bodies (Table 3).

Table 2. Small vs. large water bodies Wilcoxon rank sum test *p*-value results for VV, VH, polarized ratio, NDPI, NVHI, and NVVI. All tests are significant at an α value of 0.05.

Month	VV	VH	Polarized Ratio	NDPI	NVHI	NVVI
May	<0.001	<0.001	<0.001	<0.001	<0.001	<0.001
July	<0.001	<0.001	<0.001	<0.001	<0.001	<0.001
September	<0.001	<0.001	0.014	0.023	0.023	0.023

Table 3. Small water bodies vs. land Wilcoxon rank sum test *p*-value results for VV, VH, polarized ratio, NDPI, NVHI, and NVVI. All tests are significant for May and September at an α value of 0.05. Only VV and VH are significant for July at an α value of 0.05. Significant *p*-values (at an α value of < 0.05) are in **bold**.

Month	VV	VH	Polarized Ratio	NDPI	NVHI	NVVI
May	<0.001	<0.001	0.023	0.023	0.023	0.023
July	<0.001	<0.001	0.615	0.485	0.485	0.485
September	<0.001	<0.001	0.025	0.025	0.025	0.025

The visual analysis of boxplots comparing VV and VH backscatter data for land, small digitized peatland water bodies, and large GSW water bodies for May (Figure 4), July (Figure 5), and September 2021 (Figure 6) supported the conclusions from the Wilcoxon rank sum tests. Small peatland water bodies exhibited higher VV and VH backscatter

than large water bodies, and there was significant overlap with land samples. Most small water body VV and VH backscatter was above the Sentinel-1 noise floor of -22 dB, but large ponds exhibited VH backscatter consistently below the noise floor, representing pure specular reflectance. VH backscatter showed greater separation for the three classes than for VV.

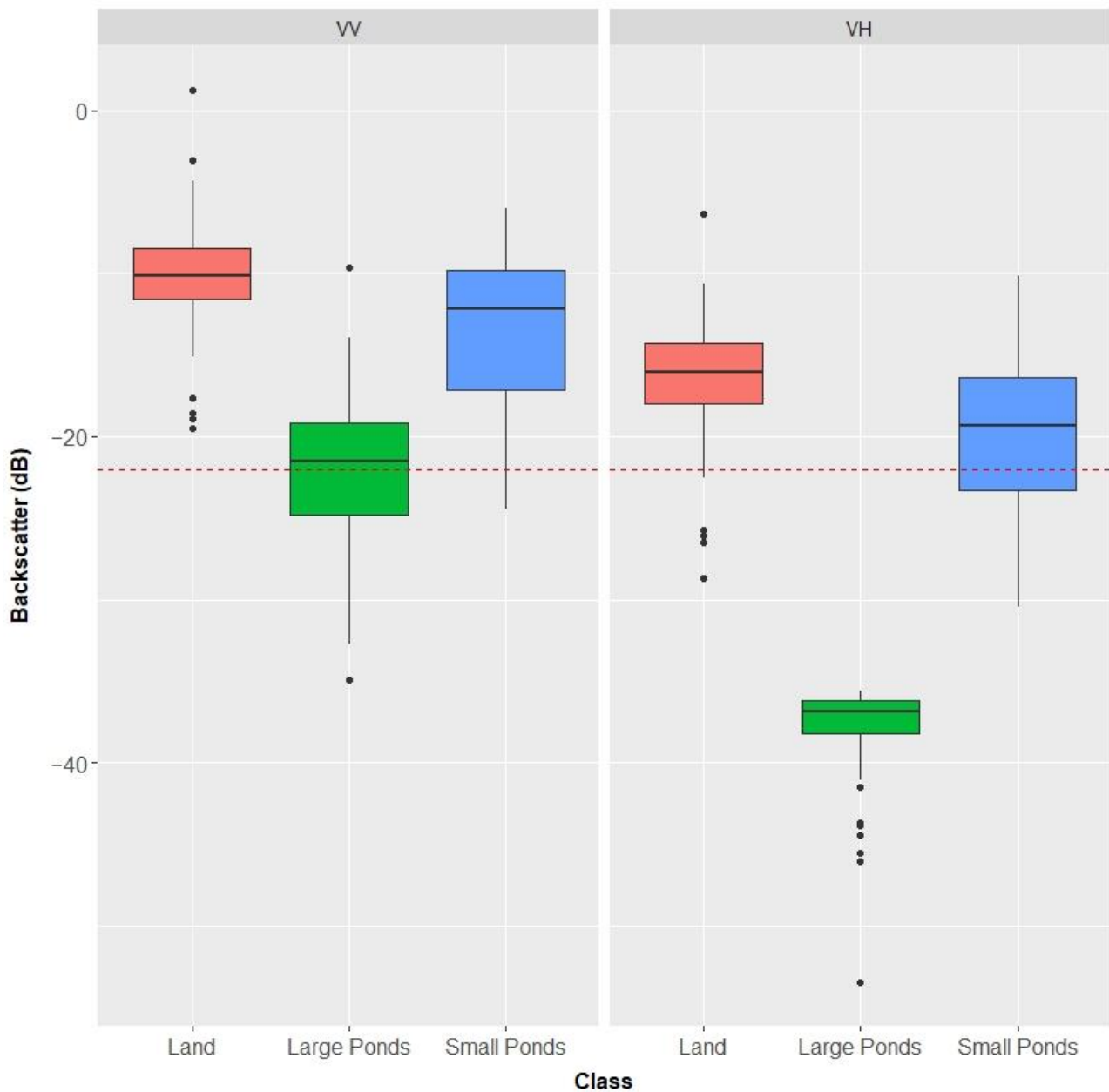


Figure 4. Boxplot showing the distribution of VV and VH for land, large GSW water bodies (large ponds), and small digitized peatland water bodies (small ponds) in May 2021. The dashed line indicates the Sentinel-1 noise floor at -22 dB.

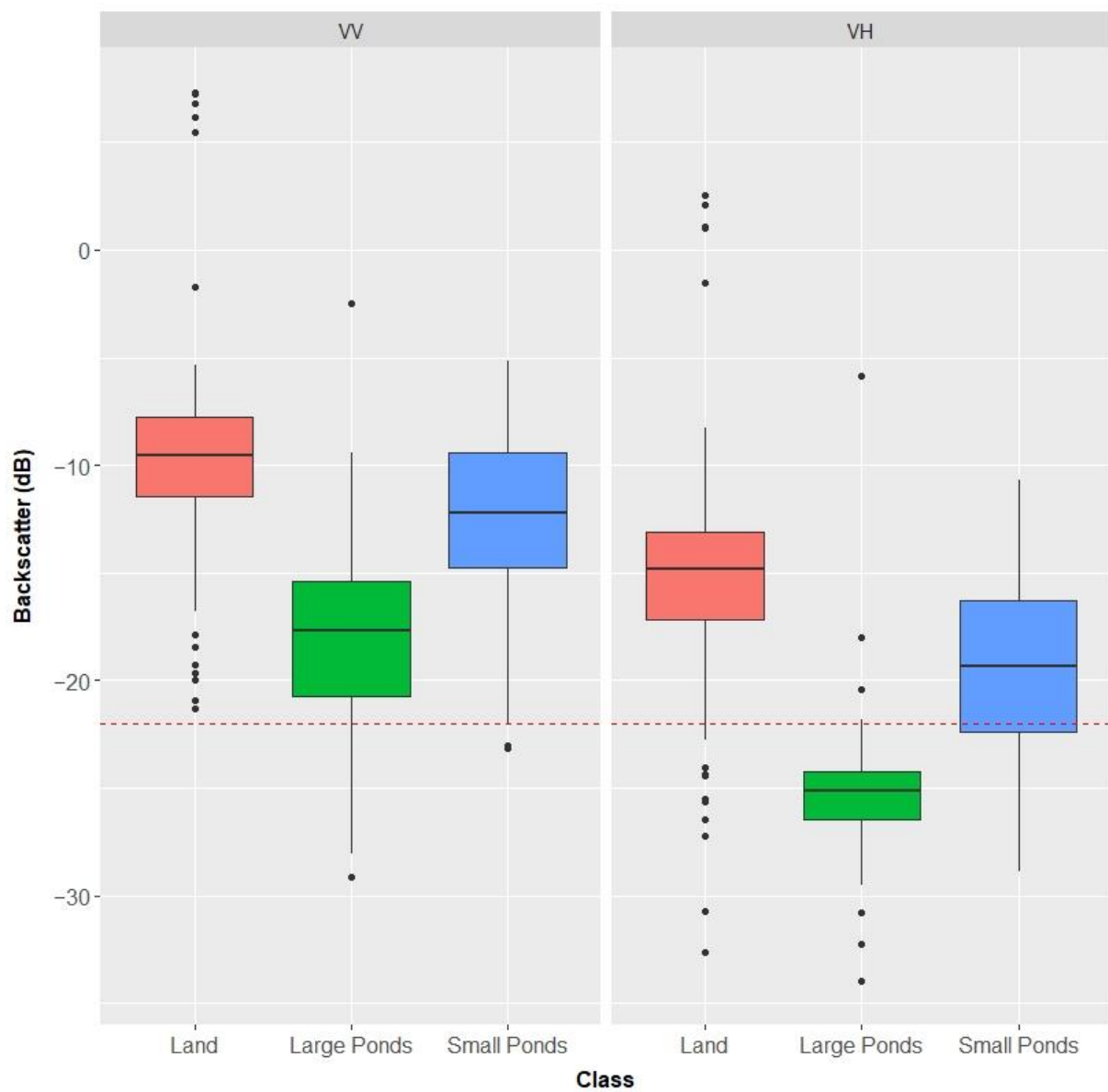


Figure 5. Boxplot showing the distribution of VV and VH for land, large GSW water bodies (large ponds), and small digitized peatland water bodies (small ponds) in July 2021. The dashed line indicates the Sentinel-1 noise floor at -22 dB.

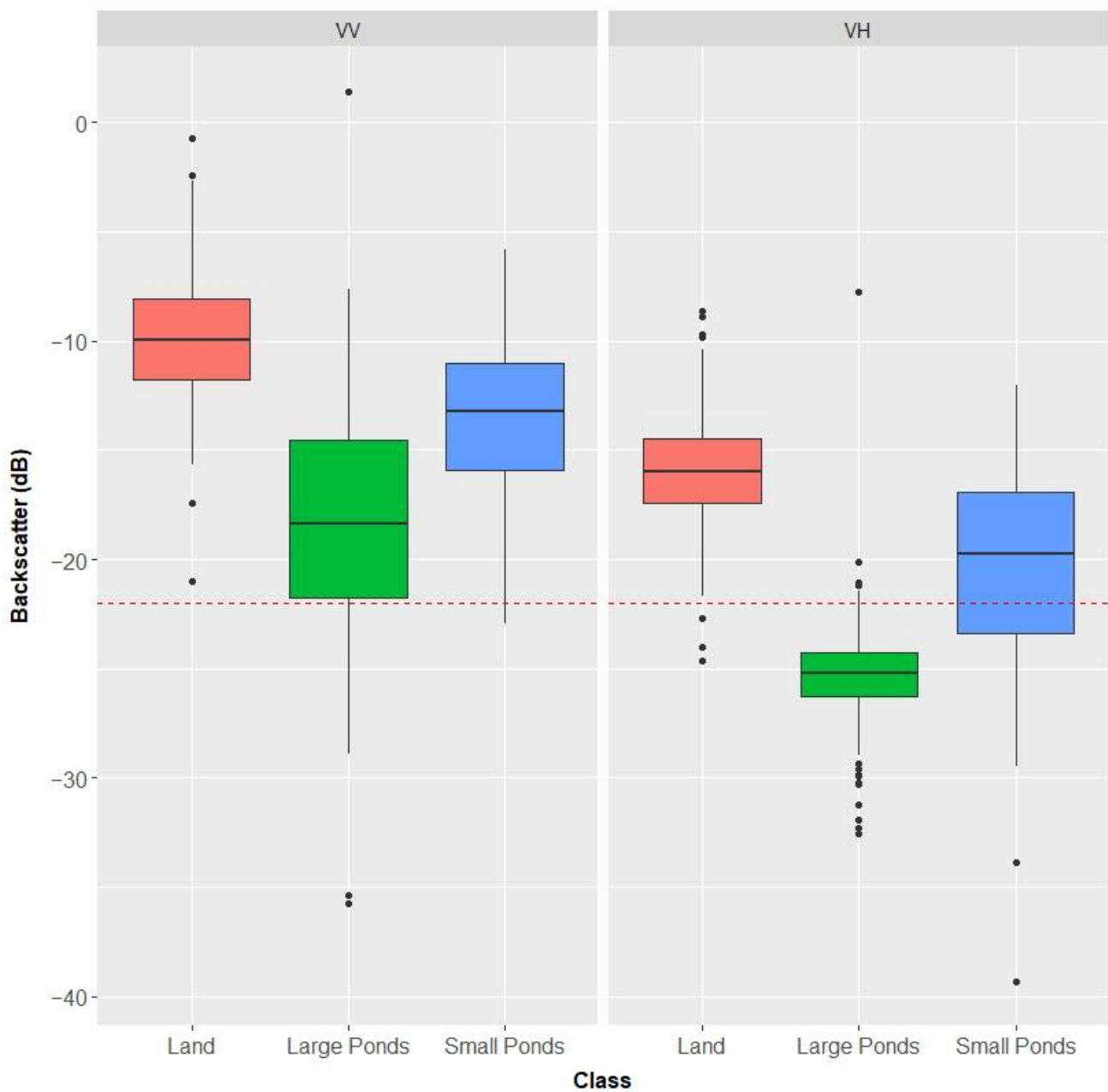


Figure 6. Boxplot showing the distribution of VV and VH for land, large GSW water bodies (large ponds), and small digitized peatland water bodies (small ponds) in September 2021. The dashed line indicates the Sentinel-1 noise floor at -22 dB.

The histogram of VV for the May extracted data set is presented below as an example to show the lack of a clear bimodal distribution in the data. The lack of a bimodal distribution indicates that there is no global threshold value that would neatly separate land and water for all sites (Figure 7). While there is a bimodal distribution present in VH between land and large water bodies (from GSW), there is no distinction between land and small digitized water bodies. These findings were consistent across the three dates tested (May, July, and September, 2021).

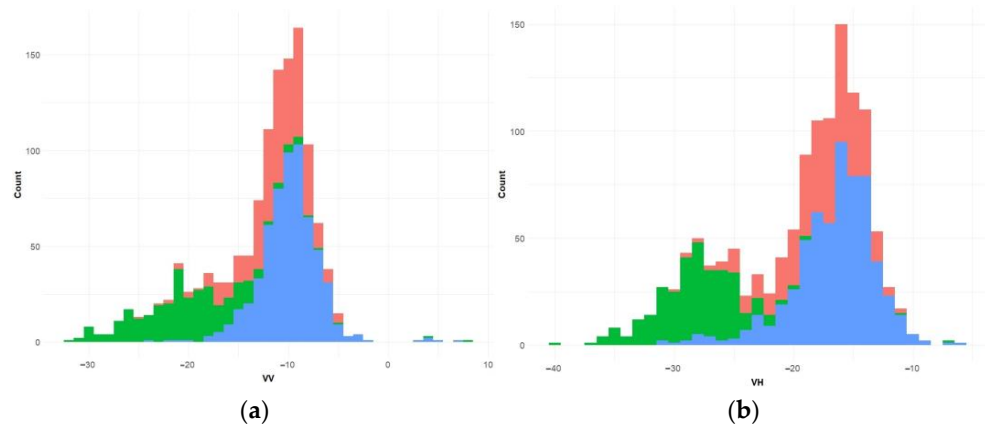


Figure 7. Histogram showing the distribution of (a) VV and (b) VH training data for land (red), large GSW water bodies (green), and small digitized peatland water bodies (blue) in May 2021.

3.3. Water Body Size and Sentinel-1 Backscatter

There are distinct groupings of water bodies on either side of the 10,000 m² area threshold (Figure 8). Linear regression revealed that there is no statistically significant relationship between water body size and backscatter. Large water bodies, which were captured in the GSW occurrence product, are 10,000 m² or larger, and have VH backscatter values below or close to the Sentinel-1 noise floor (−22 dB).

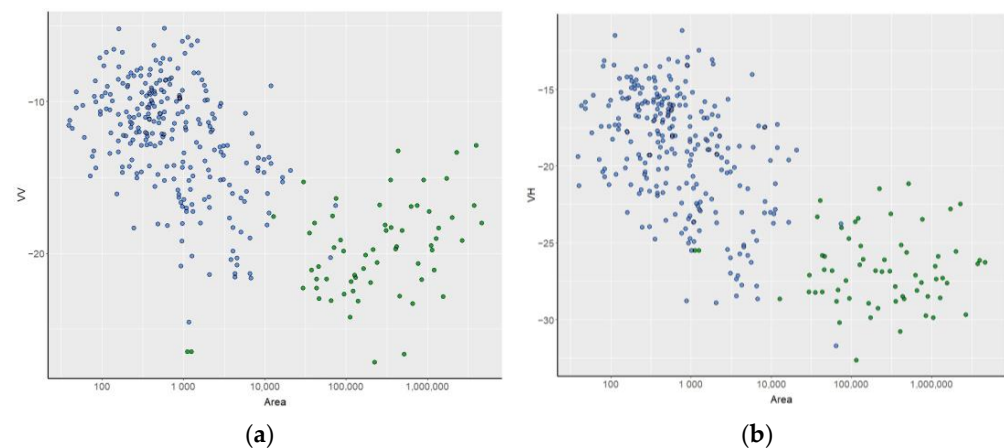


Figure 8. Scatterplot of (a) water body size (m²) vs. Sentinel-1 VV backscatter (dB) and (b) water body size (m²) vs. Sentinel-1 VH backscatter (dB) for the original collection of small water bodies (blue) across all dates combined with the secondary large water body (green) sample. Area (x-axis) scale is logarithmic.

4. Discussion

4.1. Temporally Variable Water Bodies

Peatlands represent about 12% of Canada's land mass [4]. Water bodies in these regions represent a significant area of surface water that contributes to the local and regional hydrologic cycle [6]. Maintaining a record of the variability in surface water in this region would improve meteorological forecasting, in addition to our intended purpose of wildfire susceptibility monitoring.

Existing products, such as the Global Surface Water dataset [27] and the Continental Surface Water Product [24], fall short in terms of spatial resolution, leading to the omission of small peatland water bodies. They also fall short in terms of temporal resolution, as water extent products are not produced in near real-time, meaning that products do not capture key peatland hydrologic dynamics frequently enough to be useful for wildfire monitoring. The peatland water bodies mapped in this study exhibited significant changes

over the 5-month period from May to September, where a drying trend led to water bodies shrinking or disappearing entirely over the course of a season. Changes in the number and extent of peatland water bodies over this short period support the importance of regular water mapping in peatlands in terms of both spatial and temporal resolution. With the rapid changes that small peatland water bodies exhibit, monitoring needs to occur at high frequencies and at finer spatial resolutions (<30 m). There was 62% of small peatland water bodies digitized in May, making up 13% of the total water area; these were smaller than 900 m² (sub-30 m pixel size), putting them at risk of omission due to insufficient resolution in Landsat-derived products such as the GSW dataset.

4.2. Small Water Body Backscatter Signature

The significant difference in backscatter of small and large water bodies explains why binary classifications are not sufficient to map surface water accurately. Small water bodies were distinct from land for all variables (VV, VH, and derivatives) in two of the three study periods ($p < 0.001$), and for VV and VH in all study periods. This suggests that land and small water bodies are also significantly different; however, the boxplots (Figure 4, Figure 5, Figure 6) show broad overlap between the two classes.

Threshold-based classifiers are ineffective, leading to confusion between small water bodies and land, because the actual distribution of the data is not bimodal [41]. Machine learning classifiers must make hard definitions for the relationship between variables and the output classes. This is difficult to achieve with so much overlap between land and small water bodies, particularly when small and large water bodies are treated as one class with high variance.

A Sentinel-1 based classification offers a possible solution, since it is capable of distinguishing between land and small water body classes, if representative training data can be generated. Boreal peatlands may also contain many open water bodies >100 m²; in order to cope with resolution issues, which will always be a limiting factor for accuracy, a fuzzy classification method may be implemented [42]. Sub-pixel fractional classifications have been implemented with optical data [43–45] and may be possible to implement with SAR using indices [46].

4.2.1. Multiple Scattering and Geometric Effects

The higher-than-expected backscatter values and the loose negative relationship between water body size and SAR backscatter can be explained by multiple scatterers within one pixel. Individual targets occupying the same pixel contribute to a coherent sum of scatterers, which is the same mechanism by which speckle occurs. In pixels containing water bodies less than 100 m², or for water bodies which are situated between multiple cells, the coherent sum may be influenced by highly reflective targets (e.g., emergent vegetation, to which VH polarization is particularly susceptible).

Depending on the size and positioning of a water body across the fishnet of pixels, it may be one of many targets in a given cell. In this case, the coherent sum was likely not representative of water. This effect was exacerbated by the fact that water returns very little backscatter to the sensor, so any non-water targets (e.g., emergent vegetation, land) will increase the coherent sum such that the backscatter value will not be statistically similar to water. As water body size increases, it is more likely that the center point (the points where backscatter was extracted) is in a cell that contains only water. In a cell that only contains water, the coherent sum will be representative of water.

4.2.2. Environmental Conditions

The water extent and waterbody centroids were generated from PlanetScope Super-Dove imagery [35], and the data for analysis were extracted from Sentinel-1 imagery. A mismatch of up to 9 days from the point data date to the extraction date is possible due to the differences in image collection patterns between the two sensors. Hydrologic configurations in peatlands can cause rapid changes in water level, affecting the size and depth of

peatland water bodies in short time periods [6]. It is possible that some sites in the study area could have experienced changes in water level between the date of digitization and the date of Sentinel-1 data extraction. A drop in peatland water level may expose previously submerged vegetation. Emergent vegetation in water produces high backscatter due to enhanced volumetric scattering and double bounce scattering between the surface of the water and the vegetation, especially for cross-polarized backscatter that represents volume scattering [47]. Flooded vegetation may elicit higher backscatter than non-flooded vegetation because of additional double bounce scattering from the water [48]. The opposite may also occur: water levels may rise between the date of digitization and the date of extraction, and ponds with extremely low water may have been missed in digitizing but appeared in Sentinel-1 images at a later date.

Additionally, the action of wind on water can cause waves, which increases the surface roughness. Backscatter, especially in cross-polarization, will be higher on rough water than on calm water. This may generate noise in the results and explain some outliers.

4.3. Implications of Small Peatland Water Body Omission

In the study area, the land area contained by all 100 sites was 100 km², with 0.46 km² of surface water digitized in May, when water extent was at a maximum. None of these small water bodies were captured in the GSW products, but this surface water area represented 0.46% of the total study area. While this seems like a small proportion, the Ducks Unlimited Canada Enhanced Wetland Classification contains approximately 180,000 km² of peatland [34], meaning that as much as 828 km² of surface water in peatlands identified by this classification could be omitted if using the GSW dataset as surface water reference. If this were extrapolated to all of Canada's peatlands (12% of Canada's land mass [49] or 1.2 million km²), up to 5520 km² of peatland surface water may be excluded nationally. This is a significant area of water that could be unaccounted for.

The development of improved surface water maps could have global implications. Climate and other scientific models that utilize surface water maps with similar temporal and spatial limitations to the GSW dataset will exclude large areas of water, which is likely not limited to just peatland water bodies. Management agencies that rely on these models could improve the certainty in scientific decision making and policies. A significant area of water is not currently being mapped and is potentially unaccounted for in models that rely on hydrologic data as an important component. This could give rise to misleading drought forecasts, fire risk assessments, climate models, and more.

4.4. Operationalizing Peatland Monitoring

This study demonstrates why high-quality surface water maps are not easily achievable with binary classifications. These results support the development of a Sentinel-1-based surface water classification method that meets the temporal and spatial resolution requirements to capture small peatland water bodies. With a reliable classification method that can be operationalized to become fully automated and operated in near real-time, we can achieve high-resolution monitoring of peatland surface water dynamics. Highly accurate peatland surface water mapping is a large part of peatland wildfire prediction, given the relationship between peatland health and hydrologic variability [7,22].

5. Conclusions

Fire danger monitoring will help protect Canada against the increasing risk of fire activity as a result of climate change. Present fire danger rating systems are unreliable in peatlands. Peatlands are an important carbon sink, which is a valuable resource during this period of increasing global temperatures. In order to protect peatlands from fire, we need to be able to accurately assess drought risk, which can be monitored based on changes in surface water extent. At three time periods throughout the growing season, we compared small water bodies, which were omitted from the Global Surface Water occurrence maps, to the large water bodies that were identified in existing surface water

classifications. As per the results of the Wilcoxon rank sum tests, small open water bodies exhibited distinct SAR backscatter properties from large open water bodies. Small water bodies exhibited backscatter that was higher than that for large water bodies at both co- and cross-polarizations, and were more similar to land, due to coherent sums of targets within a pixel and the varying effects of potentially mixed pixels. The samples we assessed were statistically significantly different from land for two of the three study periods. This characterization of small water body backscatter will improve the capability to produce high-quality surface water maps with SAR. These products will benefit peatland monitoring and other environments where small water bodies occur and enhance the success of applications where it is important to have an accurate quantification of surface water.

Author Contributions: Conceptualization: K.M., S.S. and S.D.; methodology: K.M., S.S. and S.D.; formal analysis: S.S.; writing—original draft preparation: S.S.; writing—review and editing: S.S., K.M., S.D. and R.C.; funding acquisition: K.M. All authors have read and agreed to the published version of the manuscript.

Funding: This research was funded by the Canadian Space Agency [grant number 21SUESULBA] and the National Sciences and Engineering Council (NSERC) [grant number RGPIN-2022-04874]. This study was also supported by Natural Resources Canada's (Canadian Forest Service) Emergency Management Strategy Wildfire Component R&D grants [grant numbers FIRENFC-24 and FIRENFC-18].

Data Availability Statement: Data are available upon request where possible.

Acknowledgments: We would like to thank Douglas Stiff and Xu Yan of the Water Survey of Canada for their support of the project. Dan Thompson of the Canadian Forest Service is thanked for great ideas and support throughout the analysis. Adam Mohiuddin is thanked for contributions to the scripts utilized for data extraction. We would like to acknowledge Planet Labs for providing access to PlanetScope imagery as a part of the Planet Education and Research Program. Thank you to Ducks Unlimited Canada for the use of the Enhanced Wetland Classification. Thank you to all the anonymous reviewers; their feedback greatly improved the quality of the manuscript.

Conflicts of Interest: The authors declare no conflict of interest. The funders had no role in the design of the study; in the collection, analyses, or interpretation of data; in the writing of the manuscript; or in the decision to publish the results.

References

1. Wieder, R.K.; Vitt, D.H. Boreal peatland ecosystems. In *Ecological Studies*; Springer: Berlin/Heidelberg, Germany, 2006.
2. Limpens, J.; Berendse, F.; Blodau, C.; Canadell, J.G.; Freeman, C.; Holden, J.; Roulet, N.; Rydin, H.; Schaepman-Strub, G. Peatlands and the carbon cycle: From local processes to global implications—A synthesis. *Biogeosciences* **2008**, *5*, 1475–1491. [[CrossRef](#)]
3. Turetsky, M.R.; Benscoter, B.; Page, S.; Rein, G.; van der Werf, G.R.; Watts, A. Global vulnerability of peatlands to fire and carbon loss. *Nat. Geosci.* **2015**, *8*, 11–14. [[CrossRef](#)]
4. Tarnocai, C. The impact of climate change on Canadian peatlands. *Can. Water Resour. J.* **2009**, *34*, 453–466. [[CrossRef](#)]
5. Lin, S.; Liu, Y.; Huang, X. Climate-Induced Arctic-Boreal Peatland Fire and Carbon Loss in the 21st Century. *Sci. Total Environ.* **2021**, *796*, 148924. [[CrossRef](#)]
6. Waddington, J.M.; Morris, P.J.; Kettridge, N.; Granath, G.; Thompson, D.K.; Moore, P.A. Hydrological feedbacks in northern peatlands. *Ecohydrology* **2015**, *8*, 113–127. [[CrossRef](#)]
7. Nelson, K.; Thompson, D.; Hopkinson, C.; Petrone, R.; Chasmer, L. Peatland-fire interactions: A review of wildland fire feedbacks and interactions in Canadian boreal peatlands. *Sci. Total Environ.* **2021**, *769*, 145212–145225. [[CrossRef](#)]
8. Benscoter, B.; Thompson, D.; Waddington, J.; Flannigan, M.; Wotton, M.; Groot, W.; Turetsky, M. Interactive effects of vegetation, soil moisture and bulk density on depth of burning of thick organic soils. *Int. J. Wildland Fire* **2011**, *20*, 418–429. [[CrossRef](#)]
9. Keane, R.E.; Burgan, R.; van Wagtenonk, J. Mapping wildland fuels for fire management across multiple scales: Integrating remote sensing, GIS, and biophysical modeling. *Int. J. Wildland Fire* **2001**, *10*, 301–319. [[CrossRef](#)]
10. Thompson, D.K.; Parisien, M.-A.; Morin, J.; Millard, K.; Larsen, C.P.S.; Simpson, B.N. Fuel accumulation in a high-frequency boreal wildfire regime: From wetland to upland. *Can. J. For. Res.* **2017**, *47*, 957–964. [[CrossRef](#)]
11. Price, D.; Alfaro, R.; Brown, K.; Flannigan, M.; Fleming, R.A.; Hogg, E.H.; Girardin, M.; Lakusta, T.; Johnston, M.; McKenney, D.; et al. Anticipating the consequences of climate change for Canada's boreal forest ecosystems. *Environ. Rev.* **2013**, *21*, 322–365. [[CrossRef](#)]
12. Coogan, S.C.P.; Robinne, F.-N.; Jain, P.; Flannigan, M.D. Scientists' warning on wildfire—A Canadian perspective. *Can. J. For. Res.* **2019**, *49*, 1015–1023. [[CrossRef](#)]

13. Thompson, D.K.; Simpson, B.N.; Whitman, E.; Barber, Q.E.; Parisien, M.-A. Peatland hydrological dynamics as a driver of landscape connectivity and fire activity in the boreal plain of Canada. *Forests* **2019**, *10*, 534. [CrossRef]
14. Price, C.; Rind, D. Possible implications of global climate change on global lightning distributions and frequencies. *J. Geophys. Res.* **1994**, *99*, 10823–10831. [CrossRef]
15. Fill, J.M.; Davis, C.N.; Crandall, R.M. Climate change lengthens southeastern USA lightning-ignited fire seasons. *Glob. Chang. Biol.* **2019**, *25*, 3562–3569. [CrossRef] [PubMed]
16. Li, Y.; Mickley, L.J.; Liu, P.; Kaplan, J.O. Trends and spatial shifts in lightning fires and smoke concentrations in response to 21st century climate over the national forests and parks of the western United States. *Atmos. Chem. Phys.* **2020**, *20*, 8827–8838. [CrossRef]
17. Hu, Y.; Fernandez-Anez, N.; Smith, T.E.L.; Rein, G. Review of emissions from smouldering peat fires and their contribution to regional haze episodes. *Int. J. Wildland Fire* **2018**, *27*, 293. [CrossRef]
18. Langmann, B.; Duncan, B.; Textor, C.; Trentmann, J.; Van der Werf, G.R. Vegetation fire emissions and their impact on air pollution and climate. *Atmos. Environ.* **2009**, *43*, 107–116. [CrossRef]
19. Page, S.E.; Siegert, F.; Rieley, J.O.; Boehm, H.D.V.; Jaya, A.; Limin, S. The amount of carbon released from peat and forest fires in Indonesia during 1997. *Nature* **2002**, *420*, 61–65. [CrossRef]
20. Liu, H.; Zak, D.; Zableckis, N.; Cossmer, A.; Langhammer, N.; Meermann, B.; Lennartz, B. Water pollution risks by smoldering fires in degraded peatlands. *Sci. Total Environ.* **2023**, *871*, 161979. [CrossRef]
21. Wu, Y.; Xu, X.; McCarter, C.P.R.; Zhang, N.; Ganzoury, M.A.; Waddington, J.M.; de Lannoy, C. Assessing leached TOC, nutrients and phenols from peatland soils after lab simulated wildfires: Implications to source water protection. *Sci. Total Environ.* **2022**, *822*, 153579. [CrossRef]
22. Waddington, J.M.; Thompson, D.K.; Wotton, M.; Quinton, W.L.; Flannigan, M.D.; Benschoter, B.W.; Baisley, S.A.; Turetsky, M.R. Examining the utility of the Canadian Forest Fire Weather Index System in boreal peatlands. *Can. J. For. Res.* **2011**, *42*, 47–58. [CrossRef]
23. Tian, X.; Mcrae, D.J.; Boychuk, D.; Jin, J.; Gao, C.; Shu, L.; Wang, M. Comparisons and assessment of forest fire danger systems. *For. Stud. China* **2005**, *7*, 53–61. [CrossRef]
24. Millard, K.; Brown, N.; Stiff, D.; Pietroniro, A. Automated surface water detection from space: A Canada-wide, open-source, automated, near-real time solution. *Can. Water Resour. J.* **2020**, *45*, 304–323. [CrossRef]
25. Schlaffer, S.; Chini, M.; Dorigo, W.; Plank, S. Monitoring Surface Water Dynamics in the Prairie Pothole Region Using Dual-Polarised Sentinel-1 SAR Time Series. *Hydrol. Earth Syst. Sci.* **2022**, *25*, 841–860. [CrossRef]
26. Harris, A. Spectral reflectance and photosynthetic properties of sphagnum mosses exposed to progressive drought. *Ecohydrology* **2008**, *1*, 35–42. [CrossRef]
27. Pekel, J.-F.; Cottam, A.; Gorelick, N.; Belward, A.S. High-resolution mapping of global surface water and its long-term changes. *Nature* **2016**, *540*, 418–422. [CrossRef]
28. Cao, H.; Zhang, H.; Wang, C.; Zhang, B. Operational Flood Detection Using Sentinel-1 SAR Data over Large Areas. *Water* **2019**, *11*, 786. [CrossRef]
29. Sass, G.Z.; Creed, I.F. Characterizing hydrodynamics on boreal landscapes using archived synthetic aperture radar imagery. *Hydrol. Process.* **2008**, *22*, 1687–1699. [CrossRef]
30. Bolanos, S.; Stiff, D.; Brisco, B.; Pietroniro, A. Operational surface water detection and monitoring using Radarsat 2. *Remote Sens.* **2016**, *8*, 285. [CrossRef]
31. Behnamian, A.; Banks, S.; White, L.; Brisco, B.; Millard, K.; Pasher, J.; Chen, Z.; Duffe, J.; Bourgeau-Chavez, L.; Battaglia, M. Semi-Automated Surface Water Detection with Synthetic Aperture Radar Data: A Wetland Case Study. *Remote Sens.* **2017**, *9*, 1209. [CrossRef]
32. Liang, J.; Liu, D. A local thresholding approach to flood water delineation using Sentinel-1 SAR imagery. *ISPRS J. Photogramm. Remote Sens.* **2020**, *159*, 53–62. [CrossRef]
33. Millard, K.; Darling, S.; Pelletier, N.; Schultz, S. Seasonally-decomposed Sentinel-1 backscatter time-series are useful indicators of peatland wildfire vulnerability. *Remote Sens. Environ.* **2022**, *283*, 113329. [CrossRef]
34. Ducks Unlimited Canada. Enhanced Wetland Classification. 2022. Available online: <https://www.ducks.ca/resources/industry/enhanced-wetland-classification-inferred-products-user-guide/> (accessed on 5 February 2023).
35. Planet Team. *Planet Application Program Interface: In Space for Life on Earth*; Planet Team: San Francisco, CA, USA, 2022. Available online: <https://api.planet.com> (accessed on 1 May 2022).
36. Gorelick, N.; Hancher, M.; Dixon, M.; Ilyushchenko, S.; Thau, D.; Moore, R. Google earth engine: Planetary-scale geospatial analysis for everyone. *Remote Sens. Environ.* **2017**, *202*, 18–27. [CrossRef]
37. Sentinel-1 SAR GRD: C-Band Synthetic Aperture Radar Ground Range Detected, Log Scaling. Earth Engine Data Catalog, Google. 2023. Available online: https://developers.google.com/earth-engine/datasets/catalog/COPERNICUS_S1_GRD (accessed on 18 April 2023).
38. Lee, J.S.; Jurkevich, L.; Dewaele, P.; Wambacq, P.; Oosterlinck, A. Speckle filtering of synthetic aperture radar images: A review. *Remote Sens.* **1994**, *8*, 313–340. [CrossRef]
39. Hogg, R.V.; Tanis, E.A. *Probability and Statistical Inference*, 7th ed.; Prentice Hall: Upper Saddle River, NJ, USA, 2006.

40. Huang, W.; DeVries, B.; Huang, C.; Lang, M.W.; Jones, J.W.; Creed, I.F.; Carrol, M.L. Automated Extraction of Surface Water Extent from Sentinel-1 Data. *Remote Sens.* **2018**, *10*, 797. [[CrossRef](#)]
41. Otsu, N. A threshold selection method from gray-level histograms. In *IEEE Transactions on Systems, Man, and Cybernetics*; IEEE: Washington, DC, USA, 1979; Volume 9, pp. 62–66.
42. Liang, P.; Yan, C. Study on mixed pixel classification method of remote sensing image based on fuzzy theory. In Proceedings of the 2009 Joint Urban Remote Sensing Event, Shanghai, China, 20–22 May 2009; pp. 1–7.
43. Rover, J.; Wylie, B.K.; Ji, L. A self-trained classification technique for producing 30 m percent-watermaps from Landsat data. *Int. J. Remote Sens.* **2010**, *31*, 2197–2203. [[CrossRef](#)]
44. Xie, H.; Luo, X.; Xu, X.; Pan, H.; Tong, X. Automated Subpixel Surface Water Mapping from Heterogeneous Urban Environments Using Landsat 8 OLI Imagery. *Remote Sens.* **2016**, *8*, 584. [[CrossRef](#)]
45. DeVries, B.; Huang, C.; Lang, M.W.; Jones, J.W.; Huang, W.; Creed, I.F.; Carroll, M.L. Automated Quantification of Surface Water Inundation in Wetlands Using Optical Satellite Imagery. *Remote Sens.* **2017**, *9*, 807. [[CrossRef](#)]
46. Tian, H.; Wang, L.; Wu, M.; Huang, N.; Li, G.; Li, X.; Niu, Z. Dynamic Monitoring of the Largest Freshwater Lake in China Using a New Water Index Derived from High Spatiotemporal Resolution Sentinel-1A Data. *Remote Sens.* **2017**, *9*, 521. [[CrossRef](#)]
47. Grimaldi, S.; Xu, J.; Li, Y.; Pauwels, V.R.N.; Walker, J.P. Flood mapping under vegetation using single SAR acquisitions. *Remote Sens. Environ.* **2020**, *237*, 111582. [[CrossRef](#)]
48. Pierdicca, N.; Pulvirenti, L.; Chini, M. *Flood Mapping in Vegetated and Urban Areas and Other Challenges: Models and Methods. Flood Monitoring through Remote Sensing*; Refice, A., D'Addabbo, A., Capolongo, D., Eds.; Springer: Cham, Switzerland, 2018.
49. Ducks Unlimited Canada and the Canadian Sphagnum Peat Moss Association Announce Partnership on World Peatlands Day. Available online: <https://www.ducks.ca/news/national/peatlands-day/> (accessed on 30 September 2022).

Disclaimer/Publisher's Note: The statements, opinions and data contained in all publications are solely those of the individual author(s) and contributor(s) and not of MDPI and/or the editor(s). MDPI and/or the editor(s) disclaim responsibility for any injury to people or property resulting from any ideas, methods, instructions or products referred to in the content.